Kent Academic Repository

Full text document (pdf)

Incipient Fault Detection for Traction Motors of High-Speed Railways Using an Interval Sliding Mode Observer

Kangkang Zhang, Bin Jiang, *Senior Member, IEEE*, Xinggang Yan, and Zehui Mao

Abstract—This paper proposes a stator-winding incipient shorted-turn fault detection method for the traction motors used in China high-speed railways. Firstly, a mathematical description for incipient shorted-turn faults is given from the quantitative point of view to preset the fault detectability requirement. Then, an interval sliding mode observer is proposed to deal with uncertainties caused by measuring errors from motor speed sensors. The active robust residual generator and the corresponding passive robust threshold generator are proposed based on this particularly designed observer. Furthermore, design parameters are optimized to satisfy the fault detectability requirement. This developed technique is applied to an electrical traction motor to verify its effectiveness and practicability.

Index Terms—Incipient fault detection; interval sliding mode observer; traction motors.

I. Introduction

AS demands for rail transportation rapidly increasing, safety and customer satisfaction have become two of the most important concerns for China Railway High-speed (CRH). To deal with these issues, intelligent vehicle fault diagnosis, fault-tolerant and monitoring techniques [1]- [4] have been developed to find out and tolerate faulty components. Traction motors are core power equipments to convert electricity into mechanical energy in electrical traction systems of high-speed railways. The sixteen traction motors in each CRH are all three-phase squirrel-cage asynchronous motors, which are the most important components to determine the riding quality. However, as claimed in [5], this kind of motors has limitations that it will result in premature incipient faults occurring on stators. The actual fault modes of stators in [5] are broken down into the following five groups: turn-to-turn, coil-to-coil, open circuit, phase-to-phase and coil-to-ground. It is turn-to-turn faults that are the initial stages and quite difficult to detect due to their incipient nature. However, the initial turn-to-turn faults may generate increasing heat, and a direct phase-to-phase or phase-to-ground faults. Thus, the motor is quickly drooped off the line. Therefore, incipient shorted-turn fault detection is essential to avoid serous failures and improve safety of high-speed railways.

Kangkang Zhang, Bin Jiang and Zehui Mao are with the College of Automation Engineering, Nanjing University of Aeronautics and Astronautics, Nanjing210016, China, e-mail: kangzhang359@nuaa.edu.cn, binjiang@nuaa.edu.cn, zehuimao@nuaa.edu.cn.
Kangkang Zhang and Xinggang Yan are with School of Engineering and Digital Arts, University of Kent, Canterbury, Kent CT2 7NT, United Kingdom, e-mail: kz51@kent.ac.uk, x.yan@kent.ac.uk.

During the past decades, rare model-based fault detection (FD) results are available for stator-winding incipient shorted-turn faults. One reason is that it is quite difficult to obtain the accurate motor faulty mathematical model and expressions of external and internal electromagnetic interferences. On the other hand, most of the traditional model-based FD strategies such as [6], [7] and [8] mainly focus on abrupt faults rather than incipient faults. Comparing with abrupt faults, incipient faults evolve more slowly and are smaller in amplitude [9], which needs FD schemes with strong detectability. In [10], the exponential function is used to characterize the small evolution rate feature for incipient faults and FD schemes with adaptive thresholds are proposed to detect the incipient faults. The methods developed in both of the two published papers [9] and [11] are aimed to deal with small evolution rate issue for incipient faults as well. However, the small amplitude feature is rarely considered in the existing FD works, even no proper mathematical description is available for incipient faults from the quantitative point of view to characterize the small amplitude feature, which motivates this paper to propose a mathematical description for incipient shorted-turn faults. Due to the small amplitude feature, stator-winding incipient shorted-turn faults are easily submerged by disturbances and uncertainties caused by measuring errors from speed sensors. Therefore, to detect incipient shorted-turn faults, particular incipient fault detection (IFD) technique should be developed to posses not only strong robustness to disturbances and uncertainties, but also strong sensitiveness to incipient shorted-turn faults.

In traditional robust FD systems such as [12] and [13], the residual generator is firstly designed and optimized to get a good trade-off between sensitivity to faults and robustness against disturbances, which is called as active robust FD in [14] where the design freedom locating only on the dynamics of residual generators can not satisfy the detectability requirements for incipient faults. Using interval observer technique proposed in [15], an alternative approach is applied to design dynamical threshold generator to produce more proper thresholds, known as passive robust FD proposed in [14]. Interval observers are proposed in [15] for the first time to estimate the set of admissible values of states, and then developed in [16], [17], [18] and [19] etc., which have been summarized in the review paper [20]. In [16], a quasi-LPV approximation for nonlinearities is built based on interval analysis and then, interval observer is designed for the quasi-LPV system using the cooperativity theory. For the planar systems with complex

poles, the time-varying interval observer is designed in [17]. In [18], the L_1/L_2 performance is introduced to design optimal interval observers for nonnegative LPV systems and for more general ones. Unobservable nonlinear systems are considered and corresponding interval observers are designed in [19]. An algorithm that propagates the uncertainties is proposed in [14] based on zonotopes and an interval linear-parameter-varying (LPV) observer is implemented to design the passive fault diagnosis method. In the passive interval observer based fault diagnosis methods, observer gains plays an important role because they determine residual sensitivities to faults and the associated adaptive thresholds derived from the uncertainties, which are analyzed in [21] detailedly. On the other hand, sliding mode techniques are not only used for control [23], [24] and [25], but also used for fault diagnosis extensively [9], [11], [22], [26], [27] and [28] because of inherent robustness to *matched uncertainties and disturbances*. Recently, sliding mode techniques are used for interval observer design such as in [22], [29] and [30] to improve the inherent robustness to matched uncertainties. High-order sliding mode techniques are used to design interval observers for LPV systems in [30], an interval sliding mode observer is constructed via a convex sum of an upper estimator and a lower estimator in [29]. Therefore, to combine interval observers and sliding mode observer techniques together to design active robust residual generators and passive robust threshold generators will be pertinent way.

Recently, an interval sliding mode observer is proposed in [22] to detect incipient sensor faults for linear time-invariant systems. Built on the author's previous work in [22], IFD schemes with detailed analysis and solid results are developed for the traction motors used in CRH in this paper. A faulty dynamical model with parameter uncertainties for the traction motors with stator-winding shorted turns is introduced from [31]. A novel quantitative mathematical description for incipient shorted-turn faults is presented via a proposed scale variable. An interval sliding mode diagnostic observer is proposed particularly for the faulty dynamical model which can compensate for *observer unmatched uncertainties* caused by measuring errors from the motor speed sensors. Then, IFD schemes, including residual generator and threshold generator, are proposed based on this diagnostic observer. Furthermore, parameters in these IFD schemes are optimized such that the fault detectability is satisfied. The contribution of this paper is summarized as follows:

1) A mathematical description for stator-winding incipient shorted-turn faults is given from the quantitative point of view.
2) A novel interval sliding mode diagnostic observer is proposed for faulty dynamical model of traction motors with uncertainties.
3) IFD schemes using active and passive robust FD techniques are proposed to satisfy the preset fault detectability requirements

Notation: In this paper, without special illustrate, $\| \cdot \|$ represents the $2-$norm of a matrix or a vector. For a real matrix or a vector M, $M > 0$ ($M \geq 0$) means that all its
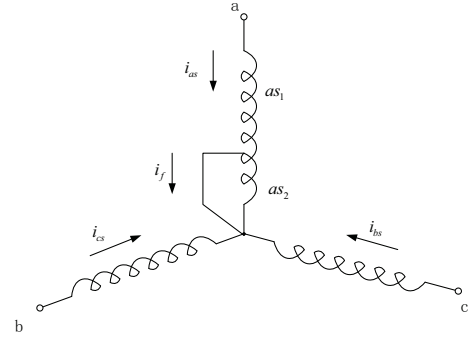

Fig. 1. Stator windings a, b, c of the traction motor with shorted-turn faults on phase a.

entries are positive (nonnegative). For any vector $x \in R^n$, $|x| = \text{col}(|x_1|, \cdots, |x_n|)$ where $x_1, \cdots, x_n$ are elements of x. For two vectors x_1, $x_2 \in R^n$ or matrices A_1, $A_2 \in R^{n \times n}$, both $x_1 \leq x_2$ and $A_1 \leq A_2$ are defined in element wise. For a matrix $A \in R^{m \times n}$ or a vector $x \in R^n$, $A^+ = \max\{0, A\}$, $A^- = A^+ - A$ and $x^+ = \max\{0, x\}$, $x^- = x^+ - x$, respectively. In addition, the symbol $\mathbf{E}_n$ represents the n-dimensional square matrix with all elements being 1.

II. PRELIMINARIES

One lemma usually used for interval observer design is shown as follows.

Lemma 1: ([30]) Let $x \in R^n$ be a vector variable satisfying $x \in [\underline{x}, \bar{x}]$ for some $\underline{x}$, $\bar{x} \in R^n$. If $A \in R^{m \times n}$ is a constant matrix, then $Ax \in [\underline{\phi}, \bar{\phi}]$ where $\underline{\phi} = A^+ \underline{x} - A^- \bar{x}$, $\bar{\phi} = A^+ \bar{x} - A^- \underline{x}$.   ∇

Then, the following lemma is introduced based on Lemma 1.

Lemma 2: Let $x \in R^n$ be a vector variable satisfying $x \in [\underline{x}, \bar{x}]$ for some $\underline{x}$, $\bar{x} \in R^n$, and $\omega \in R$ be a scalar variable satisfying $\omega \in [\underline{\omega}, \bar{\omega}]$ for some $\underline{\omega}$, $\bar{\omega} \in R$. Then $\omega x \in [\underline{\phi}, \bar{\phi}]$ where

$$\underline{\phi} = -\underline{\omega}\underline{x} + \underline{x}^+ \underline{\omega} - \underline{x}^- \bar{\omega} + \underline{\omega}^+ \underline{x} - \underline{\omega}^- \bar{x},$$
$$\bar{\phi} = -\bar{\omega}\bar{x} + \bar{x}^+ \bar{\omega} - \bar{x}^- \underline{\omega} + \bar{\omega}^+ \bar{x} - \bar{\omega}^- \underline{x} + (\bar{\omega} - \underline{\omega})(\bar{x} - \underline{x}).$$

Furthermore, if $\bar{\omega} - \underline{\omega} \leq 2\Delta\omega$, then $\omega x - \underline{\phi} \in [0, \underline{\chi}]$ and $\bar{\phi} - \omega x \in [0, \bar{\chi}]$ where

$$\underline{\chi} = (2\Delta\omega + \underline{\omega}^+)\underline{e} + \underline{\omega}^- \bar{e} + 2\Delta\omega(\underline{x}^+ + \underline{x}^-),$$
$$\bar{\chi} = (2\Delta\omega + \bar{\omega}^+)\underline{e} + (2\Delta\omega + \bar{\omega}^-)\bar{e} + 2\Delta\omega(\bar{x}^+ + \bar{x}^-)$$

with $\bar{e} = \bar{x} - x$ and $\underline{e} = x - \underline{x}$.   ∇
    Proof: See *Appendix A*.   ∎

A. Stator-Winding Shorted-Turn Faults

Stator windings a, b and c with shorted-turn faults on phase a is shown in Fig. 1 where as_2 represents the shorted turns. Denote μ as the fraction of shorted turns. Then the leakage inductance of the shorted turns is μL_{ls} where L_{ls} is the per-phase leakage inductance, and the fault impedance is resistance (R_f). Using the reference frame transformation theory presented in [32], the machine equations can then be obtained in complex dq variables as presented in [31]. Let λ_{dr} and λ_{qr} represent

stator magnetic flux linkage in dq coordinates respectively, and i_{ds} and i_{qs} represent stator currents in dq coordinates respectively. Considering the electromagnetic interferences on positive-sequence and negative-sequence currents, a fourth-order state-space presentation with single phase stator-winding shorted-turn faults is obtained by

$$\dot{\lambda}_{qr} = a_{11}\lambda_{qr} - n_p\omega_r\lambda_{dr} + a_{13}i_{qs} + f_{11}i_f, \tag{1}$$

$$\dot{\lambda}_{dr} = n_p\omega_r\lambda_{qr} + a_{22}\lambda_{dr} + a_{24}i_{ds}, \tag{2}$$

$$\dot{i}_{qs} = a_{31}\lambda_{qr} + a_{32}n_p\omega_r\lambda_{dr} + a_{33}i_{qs} + b_1v_{qs} + f_{31}i_f$$
$$+ f_{32}v_{os} + d_1(t), \tag{3}$$

$$\dot{i}_{ds} = -a_{41}n_p\omega_r\lambda_{qr} + a_{42}\lambda_{dr} + a_{44}i_{ds} + b_2v_{ds} + d_2(t), \tag{4}$$

$$y = \mathrm{col}(i_{qs}, i_{ds}) \tag{5}$$

where ω_r is the time-varying rotate speed, both $d_1(t)$ and $d_2(t)$ represent the electromagnetic interferences, $a_{11} = -\frac{1}{T_r}$, $a_{13} = \frac{L_m}{T_r}$, $f_{11} = -\frac{2\mu L_m}{3T_r}$, $a_{22} = a_{11}$, $a_{24} = a_{13}$, $a_{31} = -\frac{L_m}{\sigma L_r L_s T_r}$, $a_{32} = \frac{L_m}{\sigma L_r L_s}$, $a_{33} = -\frac{L_m^2}{\sigma L_r L_s T_r} - \frac{R_s}{\sigma L_s}$, $a_{41} = a_{32}$, $a_{42} = a_{31}$, $a_{44} = a_{33}$, $b_1 = \frac{1}{\sigma L_s}$ $b_2 = b_1$, $f_{31} = \frac{2\mu L_m^2}{3\sigma L_s L_r}\left(\frac{R_s}{L_s} - \frac{1}{T_r}\right)$, and $f_{32} = \frac{2L_m}{\sigma L_r L_s}\left(\frac{L_m}{L_s} - \frac{L_r}{L_m}\right)$ with $T_r = \frac{L_r}{R_r}$ and $\sigma = 1 - \frac{L_m^2}{L_s L_r}$.

Let $z_1 = \mathrm{col}(\lambda_{qs}, \lambda_{ds})$ and $z_2 = \mathrm{col}(i_{ds}, i_{qs})$. Then the system (1)-(4) can be written in a compact form

$$\dot{z}_1 = A_{11}z_1 + \Delta A_{11}z_1 + A_{12}z_2 + F_{12}f, \tag{6}$$

$$\dot{z}_2 = A_{21}z_1 + \Delta A_{21}z_1 + A_{22}z_2 + B_{34}v + F_{34}f + d, \tag{7}$$

$$y = C\mathrm{col}(z_1, z_2) \tag{8}$$

where $f = \mathrm{col}(i_f, v_{os})$ represents fault caused by shorted turns, $v = \mathrm{col}(v_{qs}, v_{ds})$, $d = \mathrm{col}(d_1, d_2)$ and

$$A_{11} = \begin{bmatrix} a_{11} & 0 \\ 0 & a_{22} \end{bmatrix}, \quad \Delta A_{11} = \begin{bmatrix} 0 & -n_p\omega_r \\ n_p\omega_r & 0 \end{bmatrix},$$

$$A_{21} = \begin{bmatrix} a_{31} & 0 \\ 0 & a_{42} \end{bmatrix}, \quad \Delta A_{21} = \begin{bmatrix} 0 & a_{32}n_p\omega_r \\ -a_{41}n_p\omega_r & 0 \end{bmatrix},$$

$$A_{12} = \begin{bmatrix} a_{13} & 0 \\ 0 & a_{24} \end{bmatrix}, \quad A_{22} = \begin{bmatrix} a_{33} & 0 \\ 0 & a_{44} \end{bmatrix},$$

$$F_{12} = \begin{bmatrix} f_{11} & 0 \\ 0 & 0 \end{bmatrix}, \quad F_{34} = \begin{bmatrix} f_{31} & f_{32} \\ 0 & 0 \end{bmatrix},$$

$$B_{34} = \begin{bmatrix} b_1 & 0 \\ 0 & b_2 \end{bmatrix}, \quad C = \begin{bmatrix} 0 & I_2 \end{bmatrix}.$$

It can be seen that A_{11} and A_{21} are independent of ω_r, but ΔA_{11} and ΔA_{21} rely on ω_r. It is assumed throughout this paper that the measured speed signal $\hat{\omega}_r \in \Omega_{\omega_r}$ where

$$\Omega_{\omega_r} = \{\hat{\omega}_r \in R \mid |\hat{\omega}_r - \omega_r| \le \Delta\omega_r, \ \Delta\omega_r \in R\}. \tag{9}$$

Thus, the upper bound and the lower bound of ω_r can be obtained by $\bar{\omega}_r = \hat{\omega}_r + \Delta\omega_r$ and $\underline{\omega}_r = \hat{\omega}_r - \Delta\omega_r$ respectively, and further, $\bar{\omega}_r - \underline{\omega}_r \le 2\Delta\omega_r$, $0 \le \bar{\omega}_r - \omega_r \le 2\Delta\omega_r$, $0 \le \omega_r - \underline{\omega}_r \le 2\Delta\omega_r$.

Define

$$\varphi_1 := \begin{bmatrix} 0 & -n_p \\ 0 & 0 \end{bmatrix}, \quad \varphi_2 := \begin{bmatrix} 0 & 0 \\ n_p & 0 \end{bmatrix},$$

$$\varphi_3 := \begin{bmatrix} 0 & a_{32}n_p \\ 0 & 0 \end{bmatrix}, \quad \varphi_4 := \begin{bmatrix} 0 & 0 \\ -a_{41}n_p & 0 \end{bmatrix}.$$

Then $\varphi_1 < 0$, $\varphi_2 > 0$, $\varphi_3 > 0$ and $\varphi_4 < 0$. Moreover, since $a_{32} = a_{41}$, $\varphi_3 = -a_{32}\varphi_1$ and $\varphi_4 = -a_{32}\varphi_2$. Let $\phi_1 := \omega_r z_1$. Then

$$\Delta A_{11}z_1 = \varphi_1\phi_1 + \varphi_2\phi_1, \ \Delta A_{21}z_1 = \varphi_3\phi_1 + \varphi_4\phi_1. \tag{10}$$

Based on Lemma 2, for $z_1 \in [\underline{z}_1, \bar{z}_1]$ and $\omega_r \in [\underline{\omega}_r, \bar{\omega}_r]$, there exist $\underline{\phi}_1$ and $\bar{\phi}_1$ such that $\phi_1 \in [\underline{\phi}_1, \bar{\phi}_1]$. Then

$$\varphi_1\phi_1 \in \left[\varphi_1\bar{\phi}_1, \ \varphi_1\underline{\phi}_1\right], \ \varphi_2\phi_1 \in \left[\varphi_2\underline{\phi}_1, \ \varphi_2\bar{\phi}_1\right], \tag{11}$$

$$\varphi_3\phi_1 \in \left[\varphi_3\underline{\phi}_1, \ \varphi_3\bar{\phi}_1\right], \ \varphi_4\phi_1 \in \left[\varphi_4\bar{\phi}_1, \ \varphi_4\underline{\phi}_1\right]. \tag{12}$$

A reasonable assumption in this study on f, $d_1(t)$ and $d_2(t)$ are presented as follows.

Assumption 1: There exist constants $\underline{d}$, $\bar{d}$ and $\bar{f}$ such that $\underline{d} \le d(t) \le \bar{d}$ and $\|f\| \le \bar{f}$.

Remark 1: Because the fault f in system (6)-(7) caused by shorted turns is low-frequency, the electromagnetic interferences with low frequencies are the most significant factor to influence fault detectability, which are also mainly considered in this paper. Therefore, it is also reasonable for low-frequency electromagnetic interferences d to make this assumption. In addition, the assumption for d and f in Assumption 1 is popular in interval observers and sliding mode observers (see [26], [30] and [20]). ∇

B. Incipient Shorted-Turn Fault Description

From (6)-(8), the transfer functions from f to y and from d to y are obtained respectively by $G_f(s) = C(sI - A(\omega_r))^{-1}\mathrm{col}(F_{12}, F_{34})$ and $G_d(s) = C(sI - A(\omega_r))^{-1}$ where

$$A(\omega_r) = \begin{bmatrix} A_{11} + \Delta A_{11} & A_{12} \\ A_{21} + \Delta A_{21} & A_{22} \end{bmatrix}.$$

Then, two incremental quantities, Δ_{y_f} and Δ_{y_d} caused by f and d respectively, can be described by $\Delta_{y_f} = G_f(s)f$ and $\Delta_{y_d} = G_d(s)d$. Thus,

$$\inf_{\Delta_{y_d} \ne 0} \frac{\|\Delta_{y_f}\|_2}{\|\Delta_{y_d}\|_2} = \frac{\inf_\omega \underline{\varrho}\left(G_f(j\omega)\right)}{\sup_\omega \bar{\varrho}\left(G_d(j\omega)\right)} \times \inf_{d \ne 0} \frac{\|f\|_2}{\|d\|_2}$$

where $\underline{\varrho}(\cdot)$ and $\bar{\varrho}(\cdot)$ represent the minimum and maximum singular values respectively, and ω is operating frequency of the induction motors.

Now, a scale variable to describe the developing process of incipient shorted-turn faults f is ready to be defined by

$$\Gamma = \inf_{\Delta_{y_d} \ne 0} \frac{\|\Delta_{y_f}\|_2}{\|\Delta_{y_d}\|_2} = \alpha \inf_{d \ne 0} \frac{\|f\|_2}{\|d\|_2} \tag{13}$$

where $\alpha = \inf_\omega \underline{\varrho}\left(G_f(j\omega)\right)/\sup_\omega \bar{\varrho}(G_d(j\omega))$.

Remark 2: It should be pointed out that the scale variable Γ defined in (13) provides a quantity relationship between fault f and disturbance d to some extent for traction motors. It can also be used to distinguish the incipient faults from other abrupt faults. ∇

For practical induction motors, there exist preset constants $\underline{\Gamma}$ and $\bar{\Gamma}$ such that the developing process of stator-winding shorted-turn faults is divided into three levels. The first level

is $D.1 : 0 \le \Gamma < \underline{\Gamma}$. In this case, it is unnecessary to detect the shorted-turn faults because f is small sufficiently in amplitude and the induction motor operates safely. The second level is $D.2 : \underline{\Gamma} < \Gamma < \bar{\Gamma}$. The shorted-turn faults begin to affect the normal operation and degrade the performances of motors. However, f is not large enough in amplitude so that it is challenging to detect. The third level is $D.3 : \underline{\Gamma} < \Gamma < +\infty$. In this case, the turns have become shorted seriously which even stop the running of the motors.

In this study, the shorted-turn faults belonging to $D.2$ are mainly considered, which are the so-called "incipient shorted-turn faults". A set includes all the incipient shorted-turn faults can be defined by

$$\Omega_{f,\Gamma} = \left\{ f \,\middle|\, \Gamma \in [\underline{\Gamma}, \bar{\Gamma}] \right\}. \tag{14}$$

It should be pointed out that if all $f \in \Omega_{f,\Gamma}$ are detectable, then the fault detectability of the proposed FD schemes is characterized by $\Omega_{f,\Gamma}$.

The **objective** of this paper is to design IFD schemes for the motor system (6)-(8) such that the detectability is able to be characterized by $\Omega_{f,\Gamma}$, i.e. all incipient faults $f \in \Omega_{f,\Gamma}$ are detectable, by

1) proposing an interval sliding mode diagnostic observer,
2) proposing a novel residual generator and an interval threshold generator.

III. INCIPIENT FAULT DETECTION SCHEMES

A. Interval Sliding Mode Diagnostic Observer Design

A fault diagnostic observer will be developed for system (6)-(8) in this section using interval estimation and sliding mode techniques, which will provide interval estimate for z_1 in *fault-free scenario* in the presence of uncertainty $\Delta A_{11} z_1$ and reconstruction for z_2 with uncertainty $\Delta A_{21} z_1$ and disturbance d in both *fault and fault-free scenarios*.

1) Observer Structure Design: Firstly, denote $\bar{z}_1$, $\bar{z}_2$, $\underline{z}_1$ and $\underline{z}_2$ as the estimates of upper bound and lower bound of z_1 and z_2, respectively. Based on the structure of dynamical equations in (6) and (7), the following observer structure is proposed:

$$\dot{\bar{z}}_1 = A_{11}\bar{z}_1 + \varphi_1\underline{\phi}_1 + \varphi_2\bar{\phi}_1 + A_{12}y + L_1(\bar{z}_1 - \underline{z}_1) \tag{15}$$
$$+ \bar{A}_2\mathcal{D}[t_s]\mathrm{col}(\bar{z}_2 - z_2, z_2 - \underline{z}_2) - \bar{K}_1\mathcal{D}[t_s]\nu,$$

$$\dot{\underline{z}}_1 = A_{11}\underline{z}_1 + \varphi_1\bar{\phi}_1 + \varphi_2\underline{\phi}_1 + A_{12}y - L_1(\bar{z}_1 - \underline{z}_1) \tag{16}$$
$$- \underline{A}_2\mathcal{D}[t_s]\mathrm{col}(\bar{z}_2 - z_2, z_2 - \underline{z}_2) + \underline{K}_1\mathcal{D}[t_s]\nu,$$

$$\dot{\bar{z}}_2 = A_{21}\bar{z}_1 + \varphi_3\bar{\phi}_1 + \varphi_4\underline{\phi}_1 + A_{22}\bar{z}_2 + B_{34}\nu$$
$$\underline{d} + L_2(\bar{z}_2 - \underline{z}_2) - \bar{K}_2\nu, \tag{17}$$

$$\dot{\underline{z}}_2 = A_{21}\underline{z}_1 + \varphi_3\underline{\phi}_1 + \varphi_4\bar{\phi}_1 + A_{22}\bar{z}_2 + B_{34}\nu$$
$$\bar{d} - L_2(\bar{z}_2 - \underline{z}_2) + \underline{K}_2\nu \tag{18}$$

where the initial values satisfy $\underline{z}_1(0) \le z_1(0) \le \bar{z}_1(0)$ and $\underline{z}_2(0) \le z_1(0) \le \bar{z}_2(0)$, the gain matrices $\bar{A}_2$ and $\underline{A}_2$, $\bar{K}_1$ and $\underline{K}_1$ are particularly added here to compensate for observer unmatched uncertainty, and the nonnegative matrix L_1 is used to ensure interval estimation. They will be specified later. The matrices L_2, $\bar{K}_2$ and $\underline{K}_2$ are to be designed to guarantee the occurrence of sliding mode. The nonlinear function ν is

designed as $\nu = \mathrm{col}(\mathrm{sign}(\bar{z}_2 - z_2), \mathrm{sign}(z_2 - \underline{z}_2))$. The dead-zone operator $\mathcal{D}[\cdot]$ is defined by

$$\mathcal{D}[t_s] = \begin{cases} 1, & t > t_s, \\ 0, & t \le t_s. \end{cases}$$

The time instant t_s is the time when sliding mode occurs which will be specified later.

Remark 3: The dead-zone operator $\mathcal{D}[\cdot]$ is used here to guarantee that before sliding mode occurs, the observer (15)-(16) can provide an interval estimate for z_1 by guaranteeing that $\varphi_1\underline{\phi}_1 + \varphi_2\bar{\phi}_1 + \bar{A}_2 + \mathcal{D}[t_s]\mathrm{col}(\bar{z}_2 - z_2, z_2 - \underline{z}_2) - \bar{K}_1\mathcal{D}[t_s]\nu \ge \Delta A_{11} z_1 \ge \varphi_1\bar{\phi}_1 + \varphi_2\underline{\phi}_1 - \underline{A}_2\mathcal{D}[t_s]\mathrm{col}(\bar{z}_2 - z_2, z_2 - \underline{z}_2) + \underline{K}_1\mathcal{D}[t_s]\nu$. ∇

Remark 4: It should be pointed out that the observer unmatched uncertainty caused by $\Delta A_{11} z_1$ is quite challenging to compensate. Most of related works, for example, [28], [20], [33] and [18], use robust methods such as L_1 and L_2 gains to address this issue. Different from the developed interval observer by [20] and [18] for LPV systems, a special observer structure (15)-(18) using the sliding mode technique is proposed where $\bar{K}_1\mathcal{D}[t_s]\nu$ and $\underline{K}_1\mathcal{D}[t_s]\nu$ in (15) and (16) are particularly designed to compensate for observer unmatched uncertainty caused by $\Delta A_{11} z_1$, which facilitates to improve fault detectability. ∇

2) Observer Parameters Design: Now, it is ready to design observer parameters. Firstly, throughout this paper, it is assumed that the incipient fault occurrence time instant $t_0 > t_s$, which is reasonable because t_s is adjustable. Due to the dead-zone operator $\mathcal{D}[\cdot]$, the stability analysis and interval estimation will be divided into two phases: $t \le t_s$ **phase** and $t > t_s$ **phase**. It should be noted that the $t \le t_s$ **phase** is *fault-free*. The parameter *design objective* is given as follows:

1) for $t \le t_s$, $z_1 \in [\underline{z}_1, \bar{z}_1]$, $z_1 - \underline{z}_1$ and $\bar{z}_1 - z_1$ are ultimately bounded and $\underline{z}_2$ and $\bar{z}_2$ are driven to a sliding surface.
2) for $t > t_s$, uncertainty caused by $\Delta A_{11} z_1$ is compensated for, $z_1 - \underline{z}_1$ and $\bar{z}_1 - z_1$ are still ultimately bounded, $z_1 \in [\underline{z}_1, \bar{z}_1]$ in fault-free scenario, and $\underline{z}_2$ and $\bar{z}_2$ remain on the same sliding surface in both *fault and fault-free scenarios*.

Define the estimate errors as follows:

$$\bar{e}_1 := \bar{z}_1 - z_1, \quad \underline{e}_1 := z_1 - \underline{z}_1,$$
$$\bar{e}_2 := \bar{z}_2 - z_2, \quad \underline{e}_2 := z_2 - \underline{z}_2.$$

By comparing (15)-(18) with (6)-(7), the estimate error dynamics are obtained by

$$\dot{\bar{e}}_1 = A_{11}\bar{e}_1 + \varphi_1(\underline{\phi}_1 - \phi_1) + \varphi_2(\bar{\phi}_1 - \phi_1) + L_1(\bar{e}_1 + \underline{e}_1)$$
$$+ \bar{A}_2\mathcal{D}[t_s]\mathrm{col}(\bar{e}_2, \underline{e}_2) - \bar{K}_1\mathcal{D}[t_s]\nu, \tag{19}$$

$$\dot{\underline{e}}_1 = A_{11}\underline{e}_1 + \varphi_1(\phi_1 - \bar{\phi}_1) + \varphi_2(\phi_1 - \underline{\phi}) + L_1(\bar{e}_1 + \underline{e}_1)$$
$$+ \underline{A}_2\mathcal{D}[t_s]\mathrm{col}(\bar{e}_2, \underline{e}_2) - \underline{K}_1\mathcal{D}[t_s]\nu, \tag{20}$$

$$\dot{\bar{e}}_2 = A_{21}\bar{e}_1 + \varphi_3(\bar{\phi}_1 - \phi_1) + \varphi_4(\underline{\phi}_1 - \phi_1) + A_{22}\bar{e}_2$$
$$+ (\underline{d} - d) + L_2(\bar{e}_2 + \underline{e}_2) - \bar{K}_2\nu, \tag{21}$$

$$\dot{\underline{e}}_2 = A_{21}\underline{e}_1 + \varphi_3(\phi_1 - \underline{\phi}_1) + \varphi_4(\phi_1 - \bar{\phi}_1) + A_{22}\underline{e}_2$$
$$+ (d - \bar{d}) + L_2(\bar{e}_2 + \underline{e}_2) + \underline{K}_2\nu. \tag{22}$$

Let $e_1 = \text{col}(\bar{e}_1, \underline{e}_1)$ and $e_2 = \text{col}(\bar{e}_2, \underline{e}_2)$. Then the error system (19)-(22) can be written in a compact form

$$\dot{e}_1 = A_1 e_1 + A_2 \mathcal{D}[t_s] e_2 + \Phi_1 + F_1 C_f f - K_1 \mathcal{D}[t_s] \nu, \tag{23}$$

$$\dot{e}_2 = A_3 e_1 + A_4 e_2 + \Phi_2 + \check{d} + F_2 C_f f - K_2 \nu \tag{24}$$

where $\check{d} = \text{col}(\underline{d} - d, d - \bar{d}) < 0$,

$$A_1 = \left[\begin{array}{c|c} A_{11} + L_1 & L_1 \\ \hline L_1 & A_{11} + L_1 \end{array} \right], \quad A_2 = \left[\begin{array}{c} \bar{A}_2 \\ \underline{A}_2 \end{array} \right],$$

$$A_3 = \text{diag}(A_{21}, A_{21}), \quad A_4 = \left[\begin{array}{c|c} A_{22} + L_2 & L_2 \\ \hline L_2 & A_{22} + L_2 \end{array} \right],$$

$$\Phi_1 = \left[\begin{array}{c} \varphi_1(\underline{\phi}_1 - \phi_1) + \varphi_2(\bar{\phi}_1 - \phi_1) \\ \varphi_1(\phi_1 - \bar{\phi}_1) + \varphi_2(\phi_1 - \underline{\phi}_1) \end{array} \right], \quad K_1 = \left[\begin{array}{c} \bar{K}_1 \\ \underline{K}_1 \end{array} \right],$$

$$\Phi_2 = \left[\begin{array}{c} \varphi_4(\underline{\phi}_1 - \phi_1) + \varphi_3(\bar{\phi}_1 - \phi_1) \\ \varphi_4(\phi_1 - \bar{\phi}_1) + \varphi_3(\phi_1 - \underline{\phi}_1) \end{array} \right], \quad K_2 = \left[\begin{array}{c} \bar{K}_2 \\ \underline{K}_2 \end{array} \right],$$

$F_1 = \text{diag}(F_{12}, F_{12})$, $F_2 = \text{diag}(F_{34}, F_{34})$ and $C_f = \text{col}(-I_2, I_2)$.

Recalling $\varphi_3 = -a_{32}\varphi_1$ and $\varphi_4 = -a_{32}\varphi_2$, there exists a nonsingular nonnegative matrix T_0 such that $\Phi_1 = T_0 \Phi_2$ where

$$T_0 = \frac{1}{a_{32}} \left[\begin{array}{cc} 0 & I_2 \\ I_2 & 0 \end{array} \right].$$

A new coordinate transformation $(e_1, e_2) \longrightarrow (e_s, e_2)$ where $e_s = e_1 + T e_2$ with $T = -T_0 \mathcal{D}[t_s]$ is introduced. Then

$$\dot{e}_s = (A_1 + T A_3) e_s + (A_2 \mathcal{D}[t_s] + T A_4 - (A_1 + T A_3) T) e_2 + T \check{d} + (F_1 + T F_2) C_f f - (K_1 \mathcal{D}[t_s] + T K_2) \nu, \tag{25}$$

$$\dot{e}_2 = A_3 e_s + (A_4 - A_3 T) e_2 + \Phi_2 + \check{d} + F_2 C_f f - K_2 \nu. \tag{26}$$

Remark 5: Generally speaking, it is not necessary to require T_0 to be nonnegative. However, for the considered traction motor system (6)-(8), T_0 is nonnegative, which is useful to in the following mathematical derivation. ∇

The $t \leq t_s$ **phase.** For $t \leq t_s$, $F_1 C_f f = 0$ and it follows from (23) that $\dot{e}_1 = A_1 e_1 + \Phi_1$. Based on Lemma 2, there exist $\underline{\chi}_1$ and $\bar{\chi}_1$ such that $\omega_r z_1 - \underline{\phi}_1 \in [0, \underline{\chi}_1]$, $\bar{\phi}_1 - \omega_r z_1 \in [0, \bar{\chi}_1]$. Then

$$\Phi_1 \leq \Delta A_1 e_1 + \hat{\Phi}_1 \tag{27}$$

where $\Delta A_1 = \left[\begin{array}{cc} \hat{A}_{11} & \hat{A}_{12} \\ \hat{A}_{13} & \hat{A}_{14} \end{array} \right]$ with

$$\hat{A}_{11} = \varphi_2 (2\Delta\omega_r + \bar{\omega}_r^+) - \varphi_1 \underline{\omega}_r^-,$$
$$\hat{A}_{12} = \varphi_2 (2\Delta\omega_r + \bar{\omega}_r^-) - \varphi_1 (2\Delta\omega_r + \underline{\omega}_r^+),$$
$$\hat{A}_{13} = \varphi_2 \underline{\omega}_r^- - \varphi_1 (2\Delta\omega_r + \bar{\omega}_r^+),$$
$$\hat{A}_{14} = \varphi_2 (2\Delta\omega_r + \underline{\omega}_r^+) - \varphi_1 (2\Delta\omega_r + \bar{\omega}_r^-)$$

and

$$\hat{\Phi}_1 = \left[\begin{array}{c} 2(\varphi_2 - \varphi_1)\Delta\omega_r (\underline{z}_1^+ + \underline{z}_1^-) \\ 2(\varphi_2 - \varphi_1)\Delta\omega_r (\bar{z}_1^+ + \bar{z}_1^-) \end{array} \right]. \tag{28}$$

Thus,

$$\dot{e}_1 \leq (A_1 + \Delta A_1) e_1 + \hat{\Phi}_1. \tag{29}$$

Then the following proposition is ready to be presented.

Proposition 1: If there exists a nonnegative matrix L_1 such that

1) the matrix A_1 is the Metzler matrix,
2) there exist the Hurwitz and Metzler matrix $\bar{A}_1$ satisfying $\bar{A}_1 > A_1 + \Delta A_1$,

then

(i) for $t \leq t_s$, $e_s = e_1 > 0$,
(ii) for $t \leq t_s$, $\|e_s\| = \|e_1\| < \|w_1(t)\|$ where $w_1(t)$ is ultimately bounded. ∇

Proof: Firstly, it should be noted that for $t \leq t_s$, $T = 0$ and $e_s = e_1$.

From $\underline{z}_1(0) \leq z_1(0) \leq \bar{z}_1(0)$, it is straightforward to yield that $e_1(0) \geq 0$. It follows from (11) that $\Phi_1 > 0$. Therefore, based on the positive system theory [34], with the Metzler matrix A_1, $e_1 > 0$ for $0 \leq t \leq t_s$.

Furthermore, for $t \leq t_s$, if $\bar{A}_1 > A_1 + \Delta A_1$, then it yields from $e_1 > 0$ that $\bar{A}_1 e_1 > (A_1 + \Delta A_1) e_1$. Thus, it follows from (29) that $\dot{e}_1 \leq \bar{A}_1 e_1 + \hat{\Phi}_1$. By Comparison Principle provided by [35], if $0 < e_1(0) < w_1(0)$, then $0 < e_1 \leq w_1$ where w_1 is the state of system $\dot{w}_1 = \bar{A}_1 w_1 + \hat{\Phi}_1$. Since $\bar{A}_1$ is the Hurwitz and Metzler matrix, based on positive system theory, $w_1 > 0$ and is ultimately bounded associated with $\bar{A}_1$ and $\hat{\Phi}_1$.

Hence, the result follows. ∎

Remark 6: Since ω_r is time varying, $A_1 + \Delta A_1$ is a time-varying system matrix. The stability condition for LPV systems with constant uncertain parameters developed in [18] (Theorem 7) does not work any more. In Proposition 1, the Metzler matrix $\bar{A}_1$ is introduced to deal with this problem. ∇

The $t > t_s$ **phase.** For $t > t_s$, with the parameter selection $K_1 = -TK_2$, $A_2 = -TA_4 + (A_1 + TA_3)T$, it yields from (25) that

$$\dot{e}_s = (A_1 + T A_3) e_s + T \check{d} + (F_1 + T F_2) C_f f. \tag{30}$$

Then the following Proposition is ready to be presented.

Proposition 2: If $K_1 = -TK_2$, $A_2 = TA_4 + (A_1 + TA_3)T$ and there exists a nonnegative matrix L_1 such that $A_1 + TA_3$ is the Metzler and Hurwitz matrix, then

(i) in fault-free scenario, for $t > t_s$, $e_s > 0$, $z_1 \in [\underline{z}_1, \bar{z}_1]$ and e_s is ultimately bounded,
(ii) in both fault and fault-free scenarios, for $t > t_s$, e_s is ultimately bounded and $\|e_s\| < w_2(t)$ where $w_2(t)$ is a positive scalar function determined later. ∇

Proof: It can be seen from (30) that with the selected K_1 and A_2, the observer unmatched uncertainty Φ_1 disappears, which means that it is compensated for. In fault-free scenario, based on the positive system theory [34], with the Metzler matrix $A_1 + TA_3$, $T\check{d} > 0$, $(F_1 + TF_2)C_f f = 0$ and condition $e_s(t_s) > 0$, $e_s(t) > 0$ for $t > t_s$. Since during the sliding, $e_2 = 0$, $e_1 = e_s > 0$, that is $z_1 \in [\underline{z}_1, \bar{z}_1]$. Furthermore, since $A_1 + TA_3$ is the Hurwitz matrix, e_s is ultimately bounded in both fault and fault-free scenarios.

In addition, using Comparison Principle, the reference [36] provides the method to obtain the positive scalar function $w_2(t)$ via constructing Lyapunov functions. So the construction of $w_2(t)$ is omitted here. Hence, the result follows. ∎

Since $\Phi_1 = T_0 \Phi_2$ and $T_0 \geq 0$, it follows from (27) that $\Phi_2 \leq \Delta A_3 e_1 + \hat{\Phi}_2$ where $\Delta A_3 = T_0^{-1} \Delta A_1$ and $\hat{\Phi}_2 = T_0^{-1} \hat{\Phi}_1$ with

$$T_0^{-1} = a_{32} \left[\begin{array}{cc} 0 & I_2 \\ I_2 & 0 \end{array} \right]$$

being nonnegative matrix. Then it is obtained from (26) that

$$\|\Phi_2\| \le \|\Delta A_3\| \cdot \|e_s - Te_2\| + \|\hat{\Phi}_2\|$$
$$\le \|\Delta A_3\| \cdot \|e_s\| + \|\Delta A_3 T\| \cdot \|e_2\| + \|\hat{\Phi}_2\|. \quad (31)$$

For error system (25)-(26), consider the sliding surface

$$\mathcal{S} = \{\text{col}(e_s, e_2)|e_2 = 0\}. \quad (32)$$

Next, it is focused on the design of parameters L_2 and K_2 to guarantee the reachability condition with respect to sliding surface $\mathcal{S}$ for both $t \le t_s$ *phase* and $t > t_s$ *phase* in both *fault and fault-free scenarios*. The following proposition is ready to be presented.

Proposition 3: The error system (26) is driven to sliding surface $\mathcal{S}$ in (32) before t_s and maintains on it thereafter if there exists a matrix L_2 such that

1) there exists the Hurwitz and Metzler matrix $\bar{A}_4$ such that $(\bar{A}_4)_{ii} \ge (A_4 - A_3 T + \|\Delta A_3 T\| \mathbf{E}_4)_{ii}$ and $(\bar{A}_4)_{ij} \ge |(A_4 - A_3 T + \|\Delta A_3 T\| \mathbf{E}_4)_{ij}|$ for $i, j = 1, \cdots, 4$, $i \ne j$ where $(\cdot)_{ij}$ represent the element of ith row and jth column of the matrix.
2) The gain matrix $K_2 = \lambda_{\max}(P_2) P_2^{-1} c$ where P_2 satisfies

$$\bar{A}_4^T P_2 + P_2 \bar{A}_4 < 0 \quad (33)$$

and c satisfies

$$c \ge (\|A_3\| + \|\Delta A_3\|) \max\{\|w_1(t)\|, w_2(t)\}$$
$$+ 4\|T_0^{-1}\| \cdot \|\varphi_2 - \varphi_1\|\Delta\omega_r \sqrt{\underline{z}_1^2 + \bar{z}_1^2}$$
$$+ 4 \max\{\|\bar{d}\|, \|\underline{d}\|\} + \|F_2 C_f\|\bar{f} + \eta \quad (34)$$

with η being any positive constant. ∇

Proof: It follows from Propositions 1 and 2 that $\|e_s\| \le \|w_1(t)\|$ for $t \le t_s$ and $\|e_s\| \le w_2(t)$ for $t > t_s$. Then $\|e_s\| \le \max\{\|w_1(t)\|, w_t(t)\}$ for $t \ge 0$. Since $\hat{\Phi}_2 = T_0^{-1} \hat{\Phi}_1$, $\|\hat{\Phi}_2\| \le 4\|T_0^{-1}\| \cdot \|\varphi_2 - \varphi_1\|\Delta\omega_r \sqrt{\underline{z}_1^2 + \bar{z}_1^2}$. In addition, from Assumption 1, $\check{d} \le 4 \max\{\|\bar{d}\|, \|\underline{d}\|\}$. Let $V(e_2) = \frac{1}{2} e_2^T P_2 e_2$. It is worth mentioning that based on positive system theory in [34], P_2 is a diagonal positive matrix. The time derivate of V along (26) is

$$\dot{V} = \frac{1}{2} e_2^T ((A_4 - A_3 T)^T P_2 + P_2(A_4 - A_3 T))e_2$$
$$+ e_2^T P_2 A_3 e_s + e_2^T P_2 \Phi_2 + e_2^T P_2 \check{d} + e_2^T P_2 F_2 C_f f$$
$$- e_2^T P_2 K_2 \nu$$
$$\le \frac{1}{2} e_2^T ((A_4 - A_3 T + \|\Delta A_3 T\| \mathbf{E}_4)^T P_2$$
$$+ P_2(A_4 - A_3 T + \|\Delta A_3 T\| \mathbf{E}_4))e_2 + \lambda_{\max}(P_2) \|e_2\|$$
$$\cdot \Big((\|A_3\| + \|\Delta A_3\|)\|e_s\| + \|\hat{\Phi}_2\| + \|\check{d}\| + \|F_2 C_f\|\bar{f} - c \Big)$$
$$\le \frac{1}{2} |e_2^T| (\bar{A}_4^T P_2 + P_2 \bar{A}_4)|e_2| - \lambda_{\max}(P_2) \|e_2\| \eta$$
$$\le - \sqrt{2}\eta \frac{\lambda_{\max}(P_2)}{\lambda_{\min}(P_2)} V^{\frac{1}{2}}.$$

where the first inequality is obtained based on (31) and the second inequality is obtained based on $e_2^T((A_4 - A_3 T + \|\Delta A_3 T\| \mathbf{E}_4)^T P_2 + P_2(A_4 - A_3 T + \|\Delta A_3 T\| \mathbf{E}_4))e_2 \le |e_2^T|(\bar{A}_4^T P_2 + P_2 \bar{A}_4)|e_2|$.

Therefore, the reachability condition is satisfied. Furthermore, from [37], e_2 is driven to the sliding surface $\mathcal{S}$ in (32) before t_s and maintains on it thereafter where

$$t_s = \frac{\|e_2(0)\|\lambda_{\min}(P_2)}{\eta\lambda_{\max}(P_2)}. \quad (35)$$

Hence, the result follows. ∎

Remark 7: It can be seen from (35) that the sliding mode occurrence time t_s can be reduced by decreasing $e_2(0)$ and increasing η. The value $e_2(0)$ can be adjusted by choosing appropriate initial value for the observer dynamics. The value η is the reachability which can be chosen freely. This confirms that it is reasonable to assume fault occurrence time $t_0 > t_s$. ∇

B. Residual and Interval Threshold Generation

For $t > t_s$, the sliding mode has occurred, and thus $\dot{e}_2 = e_2 = 0$, $e_1 = e_s$. Then it follows from (30) that

$$\dot{e}_1 = (A_1 + TA_3)e_1 + (F_1 + TF_2)C_f f + T\check{d}. \quad (36)$$

Remark 8: The equation (23) for e_1 can not be computed by ordinary differential equation (ODE) theory because of the existence of the discontinuous ν. It is necessary to introduce (36) such that traditional fault diagnosis methods for continuous systems can be applied. ∇

To generate residuals, an estimator $\dot{\hat{z}}_2$ for z_2 should be firstly constructed. Referring the structures of $\dot{\bar{z}}_2$ and $\dot{\underline{z}}_2$ in (17) and (18) respectively, the estimator $\dot{\hat{z}}_2$ is constructed as

$$\dot{\hat{z}}_2 = \frac{1}{2}(A_{21}(\bar{z}_1 + \underline{z}_1) + (\varphi_3 + \varphi_4)(\bar{\phi}_1 + \underline{\phi}_1)) \quad (37)$$
$$+ A_{22}\hat{z}_2 + B_{34}\nu.$$

Define $r := z_2 - \hat{z}_2$. Then *in fault scenario*, the residual generator is obtained, which, according to (26), can be expressed as

$$\dot{r} = C_r A_3 e_1 + A_{22} r + C_r(\Phi_2 + \check{d}) + F_{34} f. \quad (38)$$

where $C_r = [-\frac{1}{2}I_2, \frac{1}{2}I_2]$. To simplify the symbols, system (36) and (38) are written in a compact form

$$\dot{H} = A_H H + D_H d_H + F_H f, \quad (39)$$
$$r = C_H H \quad (40)$$

where $H = \text{col}(e_1, r)$, $d_H = \text{col}(\Phi_2, \check{d})$ and

$$A_H = \begin{bmatrix} A_1 + TA_3 & 0 \\ C_r A_3 & A_{22} \end{bmatrix}, D_H = \begin{bmatrix} 0 & T \\ C_r & C_r \end{bmatrix},$$
$$F_H = \begin{bmatrix} (F_1 + TF_2)C_f \\ F_{34} \end{bmatrix}, C_H = \begin{bmatrix} 0 & I_2 \end{bmatrix}.$$

It can be seen from (39) and (40) that the gain matrix L_1 affects both the robustness from d_H to r and sensitiveness from f to r. Reference [8] has provided a number of approaches such as H_2 to H_2 trade-off approach and H_∞ to H_- trade-off approach etc. to optimize L_1. In this paper, the optimization for L_1 is omitted and it is supposed that L_1 has been determined to satisfy the requirements in Propositions 1 and 2.

The determination of a threshold is to find out the tolerant limit for disturbances and model uncertainties under fault-free scenario [8]. Accordingly, the interval threshold should

be generated to include residual r in fault-free scenario. Two estimators $\dot{\bar{Z}}$ and $\dot{\underline{Z}}$ are firstly constructed as

$$\dot{\bar{Z}} = A_{21}\bar{z}_1 + \varphi_3\bar{\phi}_1 + \varphi_4\underline{\phi}_1 + A_{22}\bar{Z} + B_{34}v$$
$$\bar{d} + L_r(\bar{Z} - \underline{Z}), \tag{41}$$

$$\dot{\underline{Z}} = A_{21}\underline{z}_1 + \varphi_3\underline{\phi}_1 + \varphi_4\bar{\phi}_1 + A_{22}\bar{Z} + B_{34}v$$
$$\underline{d} - L_r(\bar{Z} - \underline{Z}) \tag{42}$$

where L_r is the design gain matrix to determine later. Let

$$A_Z := \left[\begin{array}{c|c} A_{22} + L_r & L_r \\ \hline L_r & A_{22} + L_r \end{array} \right]. \tag{43}$$

Then it is easy to obtain that if A_Z is the Metzler matrix, then $z_2 \in [\underline{Z}, \bar{Z}]$ in fault-free scenario.

Define $\bar{r} := \bar{Z} - \hat{z}_2$ and $\underline{r} := \underline{Z} - \hat{z}_2$. Then $r \in [\underline{r}, \bar{r}]$ in fault-free scenario. Furthermore, the threshold generator is obtained by

$$\dot{\bar{r}} = C_{\bar{r}}A_3 e_1 + C_{\bar{r}}(\Phi_2 + \check{d}) + (A_{22} + 2L_r)\bar{r}, \tag{44}$$

$$\dot{\underline{r}} = C_{\underline{r}}A_3 e_1 + C_{\underline{r}}(\Phi_2 + \check{d}) + (A_{22} + 2L_r)\underline{r} \tag{45}$$

where e_1 is determined by (36) in fault-free scenario, $C_{\bar{r}} = [\frac{1}{2}I_2, \frac{1}{2}I_2]$ and $C_{\underline{r}} = -C_{\bar{r}}$. Similar with (39)-(40), the equations (36), (44) and (45) can be written in a compact form

$$\dot{R} = A_R R + D_R d_R, \tag{46}$$
$$\mathrm{col}(\bar{r}, \underline{r}) = C_R R \tag{47}$$

where $R = \mathrm{col}(e_1, \bar{r}, \underline{r})$, $d_R = \mathrm{col}(\Phi_2, \check{d})$ and

$$A_R = \left[\begin{array}{ccc} A_1 + TA_3 & 0 & 0 \\ C_{\bar{r}}A_3 & A_{22} + 2L_r & 0 \\ C_{\underline{r}}A_3 & 0 & -A_{22} - 2L_r \end{array} \right],$$

$$D_R = \left[\begin{array}{cc} 0 & T \\ C_{\bar{r}} & C_{\bar{r}} \\ C_{\underline{r}} & C_{\underline{r}} \end{array} \right], \quad C_R = \left[\begin{array}{ccc} 0 & I_2 & 0 \\ 0 & 0 & I_2 \end{array} \right].$$

C. Incipient Fault Detectability Analysis

The objective detecting incipient faults $f \in \Omega_{f,\Gamma}$ provides the detectability requirements for these developed IFD schemes. The work in this subsection is to propose a set of sufficient conditions under which the detectability requirements are satisfied.

Denote J and J_{th} as the evaluated values of r and $\mathrm{col}(\bar{r}, \underline{r})$ respectively. In this study, as in [38],

$$J = \|r\|, \quad J_{th} = \|\mathrm{col}(\bar{r}, \underline{r})\|. \tag{48}$$

Recalling $r \in [\underline{r}, \bar{r}]$ in fault-free scenario, $J < J_{th}$ in fault-free scenario. On the other hand, to detect the incipient faults $f \in \Omega_{f,\Gamma}$, gain matrix L_r in A_R should be optimized such that J exceeds the threshold J_{th} in finite time after incipient faults occur, i.e. there is a time instant T_d with $T_d \geq t_0$ such that $J \geq J_{th}$ for $t \geq T_d$.

The calculation approach of L_r is introduced as follows: Firstly, split the r in system (39)-(40) into two components r_f and r_d caused by f and d_H respectively, i.e.,

$$r(s) = r_f(s) + r_d(s),$$
$$r_f(s) = G_{rf}(s)f(s), \quad r_d(s) = G_{rd}(s)d_H(s)$$

where $r(s)$, $r_f(s)$, $r_d(s)$ $f(s)$ and $d_H(s)$ are the Laplace transforms for $r(t)$, $r_f(t)$, $r_d(t)$, $f(t)$ and $d_H(t)$, respectively, $G_{rf}(s)$ and $G_{rd}(s)$ being transfer functions from f to r_f and from d_H to r_d respectively. Then $\|r(s)\| \geq \left| \|r_f(s)\| - \|r_d(s)\| \right| = \|r_f(s)\| - \|r_d(s)\|$ as long as $\|r_f(s)\| > \|r_d(s)\|$. Suppose that $\|r_f(s)\| > \|r_d(s)\|$. Then

$$\inf_{d_H, f} \|r(s)\| > \inf_f \|r_f(s)\| - \sup_{d_H} \|r_d(s)\|. \tag{49}$$

As stated in [38], to detect the incipient faults $f \in \Omega_{f,\Gamma}$, it requires that

$$\inf_{d_H, f} J > \sup_{d_R} J_{th}. \tag{50}$$

According to (49), a conservative condition for (50) is obtained by

$$\sup_{d_R} J_{th} \leq \inf_f \|r_f(s)\| - \sup_{d_H} \|r_d(s)\|. \tag{51}$$

It can be seen from (39) and (41) that $d_R = d_H$. Dividing d_R (or d_H) and squaring both sides of (51), it yields

$$\sup_{d_R \neq 0} \frac{J_{th}^2}{\|d_R\|^2} \leq \left(\frac{\|f\|}{\|d_H\|} \inf_{f \neq 0} \frac{\|r_f(s)\|}{\|f\|} - \sup_{d_H \neq 0} \frac{\|r_d(s)\|}{\|d_H\|} \right)^2.$$

Let $\epsilon := \frac{\|d\|}{\|d_H\|}$. Then $\frac{\|f\|}{\|d_H\|} = \frac{\epsilon\Gamma}{\alpha}$ where Γ and α are given in (13). In addition,

$$\inf_{f \neq 0} \frac{\|r_f(s)\|}{\|f\|} = \inf_{f \neq 0} \frac{\|G_{rf}(s)f(s)\|}{\|f(s)\|} = \inf_\omega \underline{\varrho}(G_{rf}(j\omega)),$$

$$\sup_{d_H \neq 0} \frac{\|r_d(s)\|}{\|d_H\|} = \sup_{d_R \neq 0} \frac{\|G_{rd}(s)d_R\|}{\|d_R\|} = \sup_\omega \bar{\varrho}(G_{rd}(j\omega)).$$

Therefore, (51) is equivalent to

$$\sup_{d_R \neq 0} \frac{\|\mathrm{col}(\bar{r}, \underline{r})\|^2}{\|d_R\|^2} \leq \gamma^2(\epsilon, \Gamma) \tag{52}$$

where $\gamma(\epsilon, \Gamma) = \frac{\epsilon\Gamma}{\alpha} \inf_\omega \underline{\varrho}(G_{rf}(j\omega)) - \sup_\omega \bar{\varrho}(G_{rd}(j\omega))$.

It should be pointed out that since z_1 is inherent bounded, $\hat{\Phi}_1$ in (28) is also bounded, which results in that $\hat{\Phi}_2$ is bounded due to $\hat{\Phi}_2 = T_0^{-1}\hat{\Phi}_1$. From Propositions 1, 2 and 3, both e_s and e_2 are both bounded. Thus, Φ_2 in d_H is bounded, and then there exists a constant $\bar{d}_H > 0$ such that $\|d_H\| \leq \bar{d}_H$. Also, from Assumption 1, $\|d\| \in [\min\{\|\bar{d}\|, \|\underline{d}\|\}, \max\{\|\bar{d}\|, \|\underline{d}\|\}]$. Thus, there exists a constant $\underline{\epsilon}$ such that $\epsilon \geq \underline{\epsilon}$ where $\underline{\epsilon} = \frac{\min\{\|\bar{d}\|, \|\underline{d}\|\}}{\bar{d}_H}$.

Therefore, based on the well-known bounded real lemma, the calculation approach for L_r is obtained as follows: the inequality (52) holds if and only if there exists a symmetric positive definite (SPD) matrix P_R, gain matrix L_r such that

$$\left[\begin{array}{cc} A_R^T P_R + P_R A_R + C_R^T C_R & P_R D_R \\ * & -\gamma^2(\epsilon, \Gamma) \end{array} \right] < 0 \tag{53}$$

holds for any $\Gamma \in [\underline{\Gamma}, \bar{\Gamma}]$ and $\epsilon \geq \underline{\epsilon}$. Hence, the following proposition is ready to be presented.

Proposition 4: All the incipient faults $f \in \Omega_{f,\Gamma}$ are detected if there exist a nonnegative matrix L_r and a SPD. matrix P_R such that A_Z defined in (43) is the Metzler matrix and (53) holds for any $\Gamma \in [\underline{\Gamma}, \bar{\Gamma}]$ and $\epsilon \geq \underline{\epsilon}$. ∇

D. Incipient Fault Detection Decision

As traditional FD in [12] and [6], the following logical relationship is used to determine the occurrence of incipient shorted-turn faults

(1) $J \le J_{th},\ \rho = 0,$

(2) $J > J_{th},\ \rho = 1.$

Therefore, *the decision on occurrence for incipient shorted-turn faults is made if* $J(T_d) > J_{th}(T_d)$ *for* $t > T_d$ where the detection time instant T_d satisfies $T_d > t_0 > t_s$. To simplify the expression, let $\rho = 0$ represent the case (1) and $\rho = 1$ case (2).

Then, the following algorithm is ready to be presented.

Algorithm 1: *The procedure to detect incipient shorted-turn faults for traction motors based on interval sliding mode diagnostic observer (15)-(18)*

Step 1: *Determine* $\bar{d},\ \underline{d}$ *and* $\bar{f}$ *in Assumption 1, and* $\bar{\Gamma}$ *and* $\underline{\Gamma}$ *to describe incipient shorted-turn faults*

Step 2: *Select* L_1 *and* L_2 *to satisfy the conditions of Propositions 1, 2 and 3*

Step 3: *Select* $\bar{K}_1,\ \underline{K}_1,\ \bar{K}_2,\ \underline{K}_2$ *and* A_2 *to satisfy the conditions in Propositions 2 and 3*

Step 4: *Select* L_r *to satisfy the conditions of Proposition 4*

Step 5: *Construct residual generator (38) and interval threshold generator (41)-(42), and then determine J and* J_{th} *by (48).*

Remark 9: Built on the authors' previous work [22], the incipient fault detection schemes with detailed analysis and solid results are developed for the traction motors used in CRH in this paper. Comparing with [22], the differences are shown as follows. The considered systems are different. A class of linear time-invariant systems is considered in [22], while in this paper, a specific traction motor system with uncertainties is considered, which is more practical. The designed fault diagnostic observers are different. Due to the uncertainties $\Delta A_{11}z_1$ and $\Delta A_{21}z_1$, in the paper, Lemma 2 is introduced to obtain interval bounds for $\Delta A_{11}z_1$ and $\Delta A_{21}z_1$, and an interval sliding mode observer structure (15)-(18) with dead-zone operator $\mathcal{D}[\cdot]$ and corresponding observer parameters L_1, L_2, $\bar{K}_1$, $\underline{K}_1$, $\bar{K}_2$, $\underline{K}_2$ and A_2 are particularly proposed and designed. ∇

IV. VERIFICATION

Following the procedure given in Algorithm 1, the incipient shorted-turn fault detection schemes are constructed as follows:

Step 1: The reference stator currents are set as $i_{qs} = 100$A and $i_{ds} = 0$A. For the traction induction motor used in CRH, electromagnetic interferences in amplitude are approximate 10% of the reference stator currents. Therefore, d_1 and d_2 in this simulation are set as

$$d_1 = 10\sin(250t)\ \text{A}, \quad d_2 = 10\cos(250t)\ \text{A}$$

and then $\bar{d}$ and $\underline{d}$ in Assumption 1 are selected as $\bar{d} = \text{col}(10, 10)$ and $\underline{d} = \text{col}(-10, -10)$.

To determine $\underline{\Gamma}$ and $\bar{\Gamma}$, the gains of $\bar{\varrho}(G_d(j\omega))$ and $\underline{\varrho}(G_f(j\omega))$ used by (13) should be given firstly through the amplitude-frequency bode diagrams of $G_d(j\omega)$ and $G_f(j\omega)$. The nominal physical parameters of the traction induction motor used in

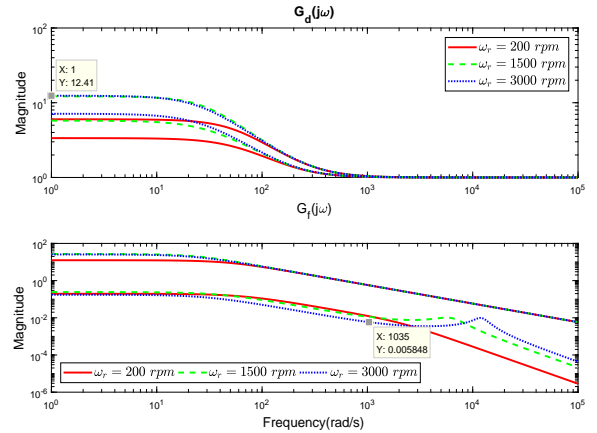| Symbol	Quantity	Value
P	Rated power	300Kw
V	Rated voltage	2500v
I	Rated current	106A
RPM	Rated rotating speed	3000rpm
L_s	stator inductance	0.0343H
L_r	rotor inductance	0.0343H
L_m	mutual inductance	0.0328H
σ	leakage factor	10.0856
R_s	stator resistance	0.114Ω
R_r	rotor resistance	0.146Ω
n_p	number of pole pairs	4

Fig. 2. Amplitude-frequency bode diagrams of $G_f(j\omega)$ and $G_d(j\omega)$.

CRH are given in Table I obtained from the traction and driving control system-fault injection benchmark (TDCS-FIB) (see [39] and [11]). In this simulation, the fraction of shorted turns is set as $\mu = 5\%$. Then the transfer functions $G_d(s)$ and $G_f(s)$ which rely on the time-varying motor speed ω_r can be obtained. However, since ω_r varies with respect to time between zero and the maximum speed 3000rpm, it is impossible to plot the amplitude-frequency bode diagrams of $G_d(j\omega)$ and $G_f(j\omega)$ for every $\omega_r \in [0, 3000\text{rpm}]$. So amplitude-frequency bode diagrams for only $\omega_r = 200$rpm, 1500rpm and 3000rpm are plotted in Fig. 2, which can describe the rough ranges for $\bar{\varrho}(G_d(j\omega))$ and $\underline{\varrho}(G_f(j\omega))$. In addition, disturbances with low frequencies affect incipient fault detection significantly because the fault-related signals caused by shorted turns are low-frequency. Therefore, we mainly focus on the frequencies belongs to $[0, 10^3\text{Hz}]$. It can be seen from Fig. 2 that

$$\sup_{\omega \in [1,10^3], \omega_r \in [0,3000]} \bar{\varrho}(G_d(j\omega)) = 12.4100,$$

$$\inf_{\omega \in [1,10^3], \omega_r \in [0,3000]} \underline{\varrho}(G_f(j\omega)) = 0.0059.$$

Thus, based on (13), $\alpha = 4.7542 \times 10^{-4}$.

For an induction motor without any asymmetry such as turn faults, the zero-sequence component of stator voltage v_{os} is zero. After incipient shorted-turn faults occur, it is assumed that v_{os} varies from 10% to 20% of the rated voltage V

given in Table I. In addition, from [31], there is a differential relationship between v_{os} and i_f that

$$\dot{i}_f = -\frac{R_s}{L_s}i_f - \frac{3v_{os}}{\mu L_s}.$$

Then the steady-state value of i_f is induced and a rough range for the incipient fault f can also be obtained by $\|f\| \in \left[1.31 \times 10^5, 2.63 \times 10^5\right]$. Thus, based on the definition of Γ given in (13), $\underline{\Gamma} = 4.4045$ and $\bar{\Gamma} = 8.8427$. Therefore, $\Omega_{f,\Gamma}$ for this induction motor is specified by $\Omega_{f,\Gamma} = \{f \mid \Gamma \in [2.2023, 4.5558]\}$.

Step 2: Considering the measuring accuracy of the speed sensors and the electromagnetic interferences imposing on the speed sensors, the measuring error in CRH is assumed to be approximate $\pm 3.5\%$ of the rated speed RPM. So the radius $\Delta \omega_r$ is chosen as $\Delta \omega_r = 105$ rpm. A closed-loop tracking control structure for the traction motor is constructed using the PID control technique to regulate the stator currents, which ensures the existences of L_1, L_2 and L_r through regulate eigenvalues of the system matrices A_{11} and A_{22}. Based on Propositions 1, 2 and 3, it can be calculated that

$$L_1 = \begin{bmatrix} 1.2940 & 2.9364 \\ 3.3982 & 1.2870 \end{bmatrix},$$

$$L_2 = \begin{bmatrix} 11.8978 & 11.3190 \\ 11.3190 & 11.8978 \end{bmatrix}.$$

Step 3: Based on Propositions 2 and 3, $\bar{K}_1$, $\underline{K}_1$, $\bar{K}_2$ and $\underline{K}_2$ are selected where $\eta = 10$ and $P_2 = 0.0081I_4$. Also, the matrix A_2 is obtained by

$$A_2 = \begin{bmatrix} -1.0684 & -1.6439 & 84.7134 & -1.6562 \\ -1.7420 & -1.0681 & -1.7298 & 84.7136 \\ 84.7303 & -1.2917 & -1.0514 & -1.2794 \\ -1.2447 & 84.7263 & -1.2570 & -1.0555 \end{bmatrix}.$$

Then the interval sliding mode diagnostic observer (15)-(18) is constructed. For simulation purpose, the zero-sequence component of stator voltage is set as $v_{os} = -250$v for $t > 2s$, which is about 10% of the rated voltage V. Thus, $f \in \Omega_{f,\Gamma}$. To verify both acceleration and uniform motions in this simulation, ω_r is set as

$$\omega_r = \begin{cases} 1000 \text{ rpm}, & t < 3, \\ 1000 + 250(t-3) \text{ rpm}, & 3 < t < 5, \\ 1500 \text{ rpm}, & t \geq 5. \end{cases}$$

Time responses of the interval sliding mode diagnostic observer are presented in Figs. 3 - 6. It is shown in Figs. 3 and 4 that before incipient faults occur, i.e., for $t < 2s$, $\bar{z}_1 - z_1 \geq 0$, $z_1 - \underline{z}_1 \geq 0$ and $\bar{z}_1 \leq z_1 \leq \underline{z}_1$. From Figs. 5 and 6, it can be seen that z_2 is driven to zero and the sliding mode occurs before 0.5s. Thus, $t_s = 0.5$s. Furthermore, after sliding mode occurs, i.e., $t > t_s$, the estimate intervals become obviously tighter in Fig. 3 than the ones for $t \leq t_s$, which verifies the effectiveness of our proposed technique to compensate for observer unmatched uncertainties $\Delta A_{11}z_1$ for the traction motors.

Step 4: With the determined gain matrix L_1, the transfer functions of $G_{rf}(j\omega)$ and $G_{rd}(j\omega)$ can be obtained and their
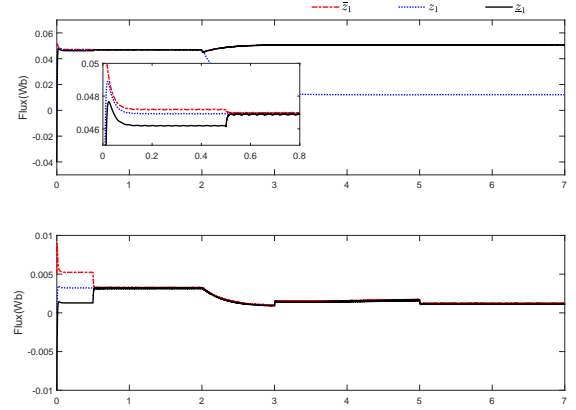

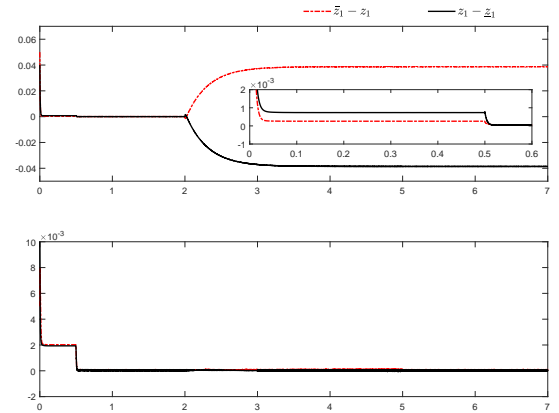Fig. 3. Time responses of $\bar{z}_1$, z_1 and $\underline{z}_1$.

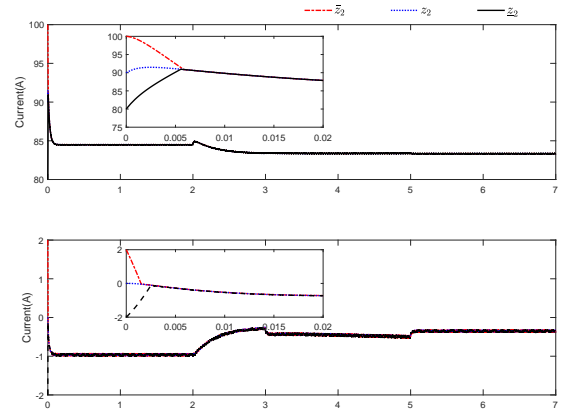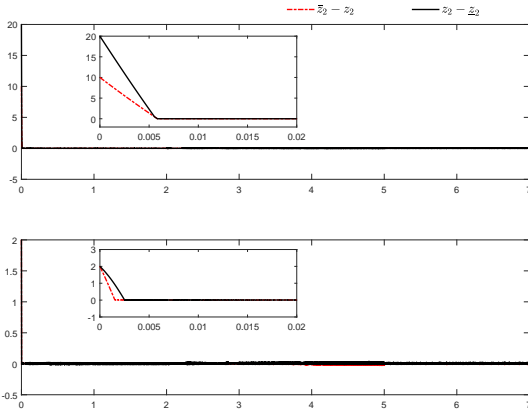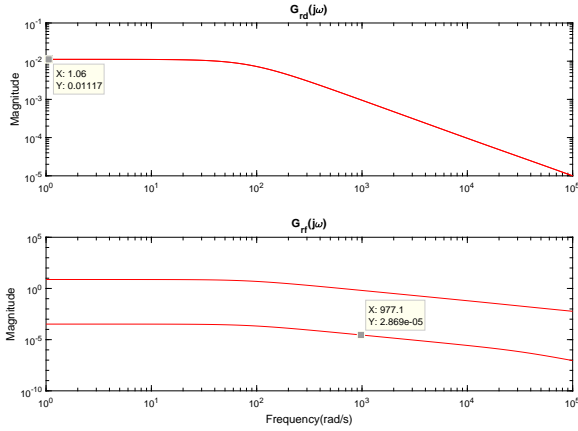Fig. 4. Time responses of $\bar{z}_1 - z_1$ and $z_1 - \underline{z}_1$.

Fig. 5. Time responses of $\bar{z}_2$, z_2 and $\underline{z}_2$.

Fig. 6. Time responses of $\bar{z}_2 - z_2$ and $z_2 - \underline{z}_2$.

Fig. 7. Amplitude-frequency bode diagrams of $G_{rf}(j\omega)$ and $G_{rd}(j\omega)$.

amplitude-frequency bode diagrams are shown in Fig. 7. Then it can obtain that

$$\sup_{\omega \in [0,10^3]} \bar{\varrho}(G_{rd}(j\omega)) = 1.117 \times 10^{-2},$$

$$\inf_{\omega \in [0,10^3]} \underline{\varrho}(G_{rf}(j\omega)) = 2.709 \times 10^{-5}.$$

From Fig. 3, the steady value of e_1 approximates zero, which implies that Φ_2 in d_H approximates zero for small sufficiently z_1. Therefore, the parameter $\underline{\epsilon} \approx 1$. Hence, based on (13),

$$\min_{\Gamma = \underline{\Gamma}, \ \epsilon = 1} \gamma^2 (\Gamma) = 0.575.$$

By solving LMI formed by (53), a feasible solution can be obtained by

$$L_r = \begin{bmatrix} 1.2256 & 3.1989 \\ 3.1975 & 1.2229 \end{bmatrix}.$$

Step 5: The residual generator based on (37) and interval threshold generator based on (41)-(42) are constructed using above calculated design parameters, and then J and J_{th} given by (48) are determined.

Time responses of r, $\bar{r}$, $\underline{r}$, J, J_{th} and ρ are presented in Figs. 8 and 9. It can be seen from Fig. 8 that r escapes from

the interval $[\underline{r}, \bar{r}]$ after 2.0s due to the fault occurrence. The residual J in Fig. 9 exceeds J_{th} at about 2.6s, and the incipient fault indicate variable ρ becomes 1 and maintains it for $t > 2.65$s. Therefore, based on the decision principle, this incipient turn fault is detected at time instant $T_d = 2.65$s.
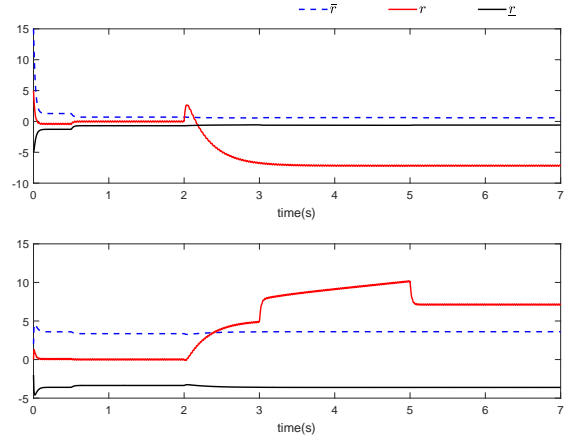
Fig. 8. Time responses of r, $\bar{r}$ and $\underline{r}$.
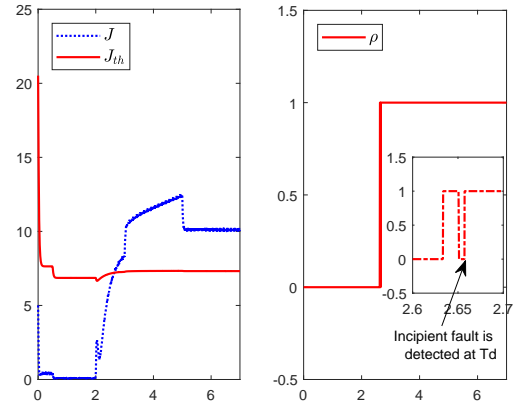
Fig. 9. Time responses of J, J_{th} and ρ.

V. Conclusion

This paper has presented a stator-winding incipient shorted-turn fault detection method for traction motors. The mathematical description of incipient shorted-turn faults has been given from the quantitative point of view. A novel interval sliding mode observer has been particularly designed as diagnostic observer to compensate for observer uncertainties caused by measuring errors from the motor speed sensors. Then, an active robust residual generator and a passive robust threshold generator have been proposed and the design parameters have also been optimized such that the considered incipient shorted-turn faults can be detected. Simulations based on a traction motor used in CRH have been presented in the paper to demonstrate the effectiveness and practicability.

Appendix A
Proof of Lemma 2

Proof: Note that ωx satisfies the following inequalities

$$
\begin{aligned}
\omega x \;-\; & \underline{\omega x} - \underline{x}\left(\omega - \underline{\omega}\right) - \underline{\omega}\left(x - \underline{x}\right) \\
= \; & \omega\left(x - \underline{x}\right) - \underline{\omega}\left(x - \underline{x}\right) \\
= \; & \left(\omega - \underline{\omega}\right)\left(x - \underline{x}\right) \geq 0, \\
\bar{\omega}\bar{x} \;-\; & \omega x - \bar{x}(\bar{\omega} - \omega) - \bar{\omega}\left(\bar{x} - x\right) + (\bar{\omega} - \underline{\omega})(\bar{x} - \underline{x}) \\
= \; & \omega\left(\bar{x} - x\right) + \bar{\omega}\left(x - \bar{x}\right) + (\bar{\omega} - \underline{\omega})(\bar{x} - \underline{x}) \\
= \; & -\left(\bar{x} - x\right)\left(\bar{\omega} - \omega\right) + (\bar{\omega} - \underline{\omega})(\bar{x} - \underline{x}) \geq 0.
\end{aligned}
$$

Then $-\underline{\omega x} + \underline{x}\omega + \underline{\omega}x \leq \omega x \leq -\bar{\omega}\bar{x} + \bar{x}\omega + \bar{\omega}x + (\bar{\omega} - \underline{\omega})(\bar{x} - \underline{x})$. Using Lemma 1 for $\underline{x}\omega$, $\underline{\omega}x$, $\bar{x}\omega$ and $\bar{\omega}x$, $\omega x \in [\underline{\phi}, \bar{\phi}]$ follows. Furthermore,

$$
\begin{aligned}
\omega x \;-\; & \underline{\phi} \\
= \; & \left(\omega - \underline{\omega}\right)\underline{e} + \underline{x}^+\left(\omega - \underline{\omega}\right) + \underline{x}^-\left(\bar{\omega} - \omega\right) + \underline{\omega}^+\underline{e} + \underline{\omega}^-\bar{e} \\
\leq \; & \left(2\Delta\omega + \underline{\omega}^+\right)\underline{e} + \underline{\omega}^-\bar{e} + 2\Delta\omega\left(\underline{x}^+ + \underline{x}^-\right)
\end{aligned}
$$

and

$$
\begin{aligned}
\bar{\phi} \;-\; & \omega x \\
= \; & -(\bar{\omega} - \omega)\bar{e} + (\bar{\omega} - \underline{\omega})(\bar{x} - \underline{x}) + \bar{x}^+\left(\bar{\omega} - \omega\right) \\
& +\bar{x}^-\left(\omega - \underline{\omega}\right) + \bar{\omega}^+\bar{e} + \bar{\omega}^-\underline{e} \\
\leq \; & \left(2\Delta\omega + \bar{\omega}^+\right)\bar{e} + \left(2\Delta\omega + \bar{\omega}^-\right)\underline{e} + 2\Delta\omega\left(\bar{x}^+ + \bar{x}^-\right).
\end{aligned}
$$

Hence, the result follows. ∎

Acknowledgment

References

[1] Y. J. Wang, Y. D. Song, H. Gao and L. Frank, Distributed fault-tolerant control of virtually and physically interconnected systems with application to high-speed trains under traction/braking failures, *IEEE Transactions on Intelligent Transportation Systems*, vol. 17, no. 2, pp. 535–545, 2016.
[2] Y. D. Song, Q. Song and W. C. Cai, Fault-tolerant adaptive control of high-speed trains under traction/braking failures: a virtual parameter-based approach, *IEEE Transactions on Intelligent Transportation Systems*, vol. 15, no. 2, pp. 737–748, 2014.
[3] S. G Gao, H. R. Dong, Y. Chen and B. Ning, Approximation-based robust adaptive automatic train control: an approach for actuator saturation, *IEEE Transactions on Intelligent Transportation Systems*, vol. 14, no.42, pp. 1733–1742, 2013.
[4] Z. H. Mao, G. Tao, B. Jiang and X. G. Yan, Adaptive compensation of traction system actuator failures for high-speed trains, *IEEE Transactions on Intelligent Transportation Systems*, vol. 18, no.11, pp. 2950–2963, 2017.
[5] A. H. Bonnett and G.C. Soukup, Cause and analysis of stator and rotor failures in three-phase squirrel-cage induction motors, *IEEE Transactions on Industry applications*, vol. 28, no. 4, pp. 921–937, 1992.
[6] J. Chen and R. J. Patton, *Robust model-based fault diagnosis for dynamic systems*, Springer Science & Business Media, New York, 1997.
[7] R. Isermann, *Fault-diagnosis systems: an introduction from fault detection to fault tolerance*, Springer Science & Business Media, Berlin, 2006.
[8] S. X. Ding, *Model-based fault diagnosis techniques: design schemes, algorithms, and tools*, Springer Science & Business Media, Berlin Heidelberg, 2008.
[9] K. K. Zhang, B. Jiang, X. G. Yan and Z. H. Mao, Sliding mode observer based incipient sensor fault detection with application to high-speed railway traction device, *ISA Transactions*, vol. 63, pp. 49–59, 2016.
[10] X. D. Zhang, T. Parisini and M. M. Polycarpou, Adaptive fault-tolerant control of nonlinear uncertain systems: an information-based diagnostic approach, *IEEE Transactions on Automatic Control*, vol. 49, no. 8, pp. 1259–1274, 2004.
[11] K. K. Zhang, B. Jiang, X. G. Yan and Z. H. Mao, Incipient voltage sensor fault isolation for rectifier in railway electrical traction systems, *IEEE Transactions on Industrial Electronics*, vol. 64, no. 8, 6763–6774, 2017.
[12] P. M. Frank, Fault diagnosis in dynamic systems using analytical and knowledge-based redundancy: A survey and some new results, *Automatica*, vol. 26, no. 3, pp. 459–474, 1990.
[13] M. Y. Zhong, S. X. Ding, J. Lam and H. B. Wang, An LMI approach to design robust fault detection filter for uncertain LTI systems, *Automatica*, vol. 39, no.3, pp. 543–550, 2003.
[14] de Oca S, Montes, V. Puig and B. Joaquim, Robust fault detection based on adaptive threshold generation using interval LPV observers, *International Journal of Adaptive Control and Signal Processing*, vol. 26, no. 3, pp. 258–283, 2012.
[15] J. L. Gouzé, R. Alain and M. Z. Hadj-Sadok, Interval observers for uncertain biological systems, *Ecological modeling*, vol. 133, no. 1, pp. 45–56, 2000.
[16] T. Raïssi, G. Videau and A. Zolghadri, Interval observer design for consistency checks of nonlinear continuous-time systems, *Automatica*, vol. 46. no. 3, pp. 518–527, 2010.
[17] F. Mazenc and O. Bernard, Asymptotically stable interval observers for planar systems with complex poles. *IEEE Transactions on Automatic Control*, vol. 55, no. 2, pp. 523–527, 2010
[18] S. Chebotarev, D. Efimov, T. Raïssi and A. Zolghadri, Interval observers for continuous-time LPV systems with L_1/L_2 performance, *Automatica*, vol. 58, pp. 82-89, 2015.
[19] G. Zheng, D. Efimov and W. Perruquetti, Design of interval observer for a class of uncertain unobservable nonlinear systems. *Automatica*, vol. 63, pp. 167–174, 2016.
[20] T. Raïssi and D. Efimov, Some recent results on the design and implementation of interval observers for uncertain systems, *Automatisierungstechnik*, vol. 66, no. 3, pp. 213–224, 2018.
[21] J. Meseguer, V. Puig, T. Escobet and J. Saludes, Observer gain effect in linear interval observer-based fault detection, *Journal of Process Control*, vol. 20, no. 8, pp. 944–956, 2010.
[22] K. K. Zhang, B. Jiang, X. G. Yan and Z. H. Mao, Incipient Fault Detection Based on Robust Threshold Generators: A Sliding Mode Interval Estimation Approach, *IFAC-PapersOnLine*, vol. 50, no. 1, pp. 5067–5072, 2017.
[23] H. Y. Li, P. Shi and D. Y. Yao, Adaptive sliding mode control of Markov jump nonlinear systems with actuator faults, *IEEE Transactions on Automatic Control*, vol. 62, no. 4, pp. 1933–1939, 2017.
[24] H. Y. Li, P. Shi, D. Y. Yao and L. G. Wu, Observer-based adaptive sliding mode control for nonlinear Markovian jump systems, *Automatica*, vol. 64, pp. 133–142, 2016.
[25] P. Shi, Y. Q. Xia, G. P. Liu and D. Rees, On designing of sliding mode control for stochastic jump systems, *IEEE Transactions on Automatic Control*, vol. 51, no. 1, pp. 97–103, 2006.
[26] C. Edwards, S. Spurgeon and R. J. Patton, Sliding mode observers for fault detection and isolation, *Automatica*, vol. 36 36, no. 4, pp. 541–553, 2000.
[27] X. G. Yan and C. Edwards, Nonlinear robust fault reconstruction and estimation using a sliding mode observer, *Automatica*, vol. 43, no. 9, pp. 1605–1614, 2007.
[28] H. Alwi, C. Edwards and C. P. Tan, Sliding mode estimation schemes for incipient sensor faults, *Automatica*, vol. 45, no. 7, pp. 1679–1685, 2009.
[29] H. Oubabas, S. Djennoune, Said and M. Bettayeb, Interval sliding mode observer design for linear and nonlinear systems, *Journal of Process Control*, vol. 61, pp. 12–22, 2018.
[30] D. Efimov, L. Fridman, T. Raïssi, A. Zolghadri and R. Seydou, Interval estimation for LPV systems applying high order sliding mode techniques. *Automatica*, vol. 48, no. 9, pp. 2365–2371, 2012.
[31] R. M. Tallam, G. H. Thomas and G. H. Ronald, Transient model for induction machines with stator winding turn faults, *IEEE Transactions on Industry Applications*, vol. 38, no. 3, pp. 632–637, 2002.

[32] P. Krause, O. Wasynczuk, S. D. Sudhoff and S. Pekarek, *Analysis of electric machinery and drive systems*, John Wiley & Sons, 2013.

[33] C. P. Tan and C. Edwards, Sliding mode observers for robust detection and reconstruction of actuator and sensor faults, *International Journal of Robust and Nonlinear Control*, vol. 13, no. 5, pp. 443–463, 2003.

[34] L. Farina and R. Sergio, *Positive linear systems: theory and applications*, John Wiley & Sons, New York, 2011.

[35] H. K. Khalil, *Nonlinear systems*, Prentice Hall, New Jewsey, 2002.

[36] X. G. Yan and C. Edwards, Robust sliding mode observer-based actuator fault detection and isolation for a class of nonlinear systems, *International Journal of Systems Science*, vol. 39, no. 4, pp. 349–359, 2008.

[37] C. Edwards and S. Spurgeon, *Sliding mode control: theory and applications*, CRC Press, London, 1998.

[38] E. M. Abbas, M. M. Akhter and S. M. Rock, Effect of model uncertainty on failure detection: the threshold selector, *IEEE Transactions on Automatic Control*, vol. 33, no. 12, pp. 1106–1115, 1988.

[39] C. H. Yang, C. Yang, P. Tao, X. Y. Yang and W. H. Gui, A fault-injection strategy for traction drive control systems, *IEEE Transactions on Industrial Electronics*, vol. 64, no. 7, pp. 5719–5727, 2017.

Zehui Mao received the Ph.D. degree in control theory and control engineering from Nanjing University of Aeronautics and Astronautics, Nanjing, China, in 2009. She is currently an Associate Professor with the College of Automation Engineering, Nanjing University of Aeronautics and Astronautics. She is also a Visiting Scholar with the University of Virginia. She was involved in the area of fault diagnosis, with particular interests in nonlinear control systems, sampled-data systems and networked control systems. Her research interests include fault diagnosis and fault-tolerant control of systems with disturbance and incipient faults, and high speed train and spacecraft flight control applications.

Kangkang Zhang received the B.Sc. degree in automatic control from Henan University of Technology, Henan, China in 2008, M.Sc. degree in control theory and control engineering from Northeastern University, Shenyang, China in 2014. He is now a Ph.D. student at the College of Automation Engineering, Nanjing University of Aeronautics and Astronautics, Nanjing, China, and also a visiting Ph.D. student at School of Engineering and Digital Arts, University of Kent, Canterbury, United Kingdom. His research interests cover fault diagnosis and fault-tolerant control, sliding mode observer and control, interval observer and adaptive estimation and their applications in high-speed trains.

Bin Jiang received the Ph.D. degree in automatic control from Northeastern University, Shenyang, China, in 1995. He had been a Post-Doctoral Fellow, a Research Fellow and a Visiting Professor in Singapore, France, USA, and Canada, respectively. He is currently a Chair Professor of the Cheung Kong Scholar Program, Ministry of Education, and the Dean of College of Automation Engineering, Nanjing University of Aeronautics and Astronautics, China. His research interests include fault diagnosis and fault-tolerant control and their applications in aircraft, satellite and high-speed trains. He is an Associate Editor or Editorial Board Member for a number of journals, such as IEEE TRANSACTION ON CONTROL SYSTEMS TECHNOLOGY, International Journal of Control, Automation and Systems, Nonlinear Analysis, Hybrid Systems, Acta Automatica Sinica, Journal of Astronautics; Control and Decision, and Systems Engineering and Electronics Technologies.

Xing-Gang Yan received the B.Sc. degree from Shaanxi Normal University in 1985, the M.Sc. degree from Qufu Normal University in 1991, and the Ph.D. degree in engineering from Northeastern University, China, in 1997. He was a Lecturer with Qingdao University, China, from 1991 to 1994. He was a Research Fellow/Associate with the University of Hong Kong, China, with Nanyang Technological University, Singapore, and with University of Leicester, U.K. He is currently a Senior Lecturer with University of Kent, U.K. He is the Editor-in-Chief of International Journal of Engineering Research and Science & Technology. His research interests include sliding mode control, decentralised control, fault detection and isolation, and control and observation of nonlinear systems and time delay systems with applications.